Iranian Journal of Hydrogen & Fuel Cell 1(2020) 13-31

Iranian Journal of Hydrogen & Fuel Cell

IJHFC

Journal homepage://ijhfc.irost.ir

Exergy and Energy Analysis of Effective Utilization of Carbon Dioxide in the Gas-to-Methanol Process

Nima Norouzi[a] Saeed Talebi[b,*]

[a] Department of energy engineering and physics, Amirkabir university of technology (Tehran polytechnic), 424 Hafez Avenue, P.O. Box 15875-4413, Tehran, Iran, sa.talebi@aut.ac.ir

[b] Department of energy engineering and physics, Amirkabir university of technology (Tehran polytechnic), 424 Hafez Avenue, P.O. Box 15875-4413, Tehran, Iran, nima1376@aut.ac.ir

Article Information

Article History:

Received:
2020-03-23
Received in revised form:
2020-04-10
Accepted:
2020-04-14

Keywords

Greenhouse gas
Carbon dioxide utilization
Methanol
Exergy analysis

Abstract

Two process models are used to convert carbon dioxide into methanol. These processes have been extended and improved using Aspen Plus simulator software. Both processes are found in the CO_2 correction system. In this machine, the desired synthesis gas is produced in a flexible configuration. At the same time, the conversion of $CO_2$to hydrogen via a copper-based catalyst has been accomplished in the methanol blending and bonding machine to produce the target product, methanol. The simulation results show that, in both proposed CO_2-gas-to-methanol process, the energy efficiency can be significantly increased, and the CO_2 emission significantly reduced as compared to the conventional Gas-to-methanol process. Energy efficiency is also affected by the recycling factor. The higher the recycling factor, the better the CO_2 conversion and reaction will be as well as increased energy efficiency and decreased CO_2 emission. However, the refractive index seems to have little effect on energy efficiency, and the useful recovery that goes back to the breeder is meager. Implementation of the carbon dioxide utilization process for gas-to-methanol units has significant impacts on these systems in the term of energy and exergy, the performance ratios increased 6.5 and 4.2%, respectively, compared to the base cases. Regarding exergoeconomics, the exergy cost rate decreased 71 $/s. An exergoenvironmental analysis showed the impacts are significant. The environmental impact difference increased by 3%, which, because of its definite form, means a carbon dioxide utilization plant makes a more significant positive difference in the environment.

1. Introduction

The process of converting methanol to methanol (GTM) based on methanol synthesis and mixing has attracted much attention in the last decade, as demand for methanol is generally increasing and the natural gas supply is relatively low [1].

Methanol is one of the essential raw materials for the petrochemical and energy industry. The reason is the widespread use of matter [2]. Its use ranges

*Corresponding author: satalebi@aut.ac.ir, sa.talebi2015@gmail.com

from chemistry (as a solvent or raw material for the production of olefins, formaldehyde, acetic acid, etc.) to the energy industry (as a fuel, in combination with diesel, and for use in fuel cells). Methanol is widespread and will potentially become a more valuable commodity in the coming years. This can be attributed to the abundance of natural gas resources, such as shale gas and methane on the coal bed, that has recently received much attention in horizontal fissures and hydraulic fission technology [3].

The main human impacts on CO_2 emissions in nature can be described as the leading global warming factor [3]. Various technologies to reduce CO_2 emissions are being developed and implemented such as carbon capture and storage technology (CCS) as well as carbon capture and use technology (CCU) [4]. Comparing the two seems to be a useful and cost-effective CCU. Because it not only reduces CO_2 emissions, it can also produce valuable fuels and chemicals that reduce the cost of petrochemical plants to produce and convert CO_2 [5]. The CCU approach to convert CO_2 to hydrogen and modify CO_2 has recently been considered as a promising way to use CO_2, given its potential for use in the GTM process at large units. GTM technology can also use natural and greenhouse gas wastes [6]. These gases are released due to their low economic value and generate a large amount of excess CO_2.

The GTM process, based on methanol synthesis and bonding, generally consists of three parts: first, the production of gas in which the methane correction reaction is assisted by processes such as automatic heat correction (ATR), partial methane oxidation reaction (POM), methane steam reforming (SMR), and methane carbon dioxide reforming (CDR) [7]. Second, the synthesis and repair of methane usually carried out by a copper-based catalyst, which eventually produces crude methanol with a small number of other products such as dimethyl ether (DME) and ethanol. Third, product purification, which separates out the final product, methanol. The current methane correction technology mentioned above has several problems [8]. The ratio $H_2/(2CO + 3CO_2)$ deviates from the value of one, but we need that value for the methanol compound. Thus, an adjustment step is required for the addition of the coefficient $H_2/(2CO + 3CO_2)$This modification, which is expensive, is also required for POM and ATM processes [9].

Therefore, in the present study, two modification reactions of methane have been made to adjust the $H_2/(2CO+3CO_2)$ ratio to produce synthetic gas. Extensive efforts have recently been made to improve the GTM process based on methanol compounding. Ehlinghter and his colleagues have investigated the design, analysis, and integration of the methanol process from shale gas [10]. Bermudez and his colleagues have stimulated the production of methanol from a coal-fired stove that is the basis for CO_2 correction [11]. Lee and his colleagues designed processes with three models for gas-to-liquid (GTL) production that produce methanol, DME, F-T diesel. They did this to determine the best GTL process with a low-priced scenario. Park and his colleagues studied the best reaction conditions for maximum methanol production [12].

Several processes have been designed and simulated to compare GTM processes based on methanol synthesis and to identify the most desirable and cost-effective. Others have looked at all stages of the GTM process and considered their energy efficiency and CO_2 emissions [13]. Building on studies on FTs based on the GTL process that uses iron and cobalt as catalysts, we proposed two new methods for the GTM process, which we call CGTMs [14]. The base of the methanol compound functions and the CO_2 is reacted and converted to it by two hydrogen conversion and conversion reactions. This process has shown an increase in energy efficiency as well as a decrease in CO_2 emission, which is due to the recycling of the reactive part of the synthesized gas and its return to the methanol correction and recovery apparatus [15].

Table 1. Nomenclature of the text.

Air Separation Unit	ASU
Thermal car modification	ATR
Capital costs	CAPEX
Carbon capture and storage	CCS
Carbon capture and operation	CCU
Optimal carbon dioxide from methane	CDR
Carbon formation reaction	CFR
Carbon dioxide utilization process from gas to methanol	CGTM
Carbon efficiency	C_{eff}
Dimethyl ether	DME
Fischer-Tropsch	F-T
Gas to liquid	GTL
Gas to methanol	GTM
Langmuir-Hinshelwood-Hougen-Watson	LHHW
Lower thermal value	LHV
natural gas	NG
Operating costs	OPEX
Partial oxidation of methane	POM
Methane correction with water vapor	SMR
Steam to carbon	S/C
Thermal efficiency	Teff
Water vapor changes	WGS
Thermal Exergy efficiency	Texe
Carbon exergy efficiency	Cexe

A literature review shows some significant gaps in the body of methanol-based carbon-dioxide-utilization or the CDU field of research and technology: 1. methanol-based CDU has not been getting enough attention in recent papers [5], 2. the gas-to-methanol process can be made more sustainable [7], and 3. the energy and exergy performance of the GTM process is relatively low [14]. In this regard, the main aim of this paper is to suggest a combination of the CDU with conventional GTM technology to resolve these issues. Moreover, considering all the mentioned facts, the main innovations of this paper are:

- Implementation of an Exergy-based design for a GTM process
- Improvement of the energy and exergy
- performance of the unit
- Combination of the CDU and GTM units into a CGTM unit
- Designation of a sustainable green methanol supply-chain

2. Methods and materials

In general, the GTM process based on methanol composition includes a primary feeder, gas pre-treatment, correction device, methanol mixer, and crop separator. However, current studies do not generally include gas pre-treatment and separation devices because they have performed well in petrochemical plants, with little impact on process efficiency [15]. We now examine CGTM process models in a simple but meaningful way, which

necessarily includes feeding, breeding, methanol mixing, and recycling devices with several separation lines. The difference between theproposed GTM and CGTM is in the structure of the process, which can be seen in Figure 1 [13].

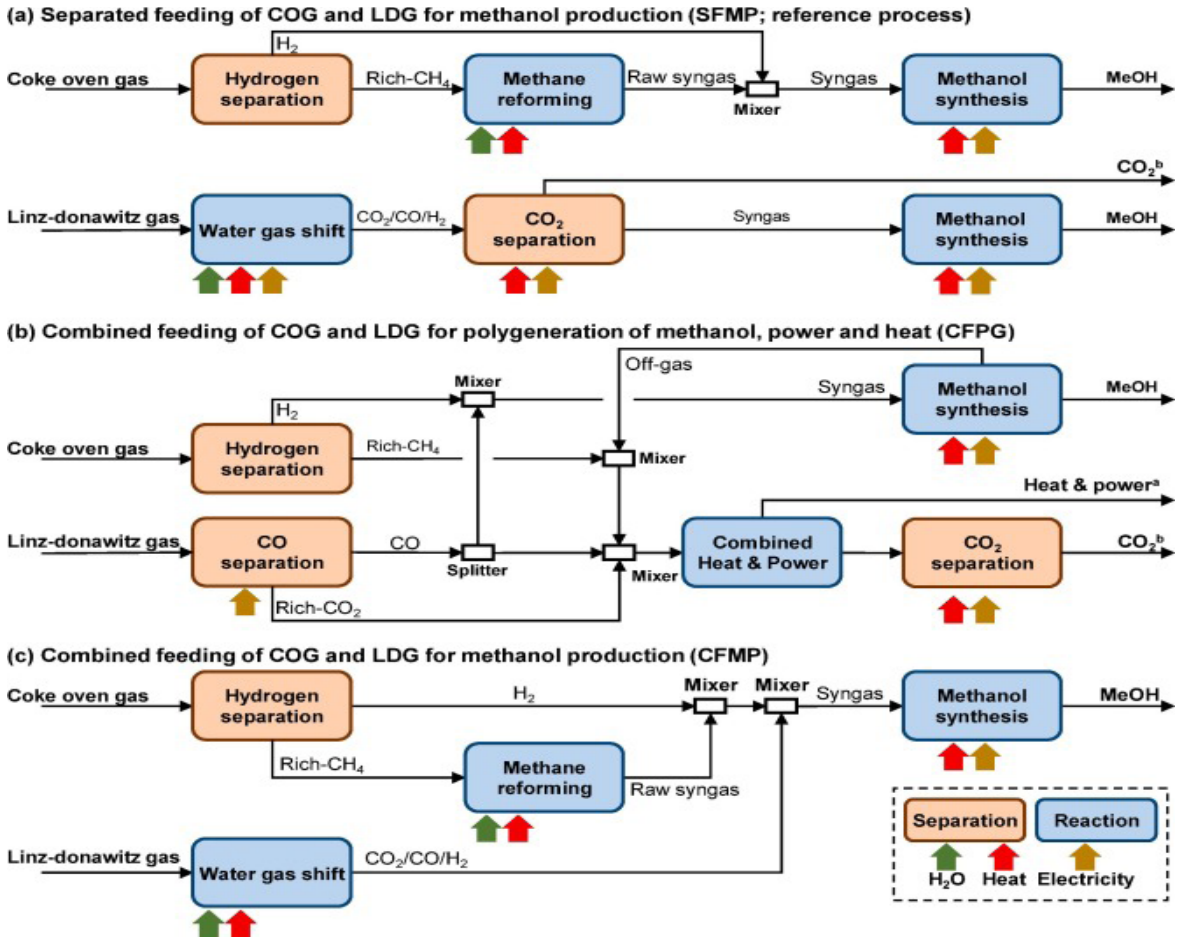

Figure 1. Schematic of the CGTM flow chart process [7, 11, 13, 15].

(1) In Option 1, we first modify CO_2 with natural gas and water vapor to produce a synthesis gas and CO_2 mixed with steam, and then convert the methanol to hydrogen and convert CO_2 [16].

(2) In Option 2, we deliver fresh CO_2 directly to the methanol mixing plant to produce our desired methanol utilizing CO_2 hydrogen conversion. Several underlying assumptions have been made with the models used, which we will explain below [11].

Methane, ethane, butane, propane, CO_2, and N_2 are used as the main components of primary nutrition, and we call them natural gas (NG). The thermodynamic methods used for both models are based on the Peng Robinson relation, which results in noble gases, hydrocarbons, and alcohols. In the correction device, previous modifiers were used for the primary modifier, which operated at 550 ° C and 5 bar. In this case, the Ni catalyst in the modifier converts almost all of the C_2 + hydrocarbons present in the NG, and then converts the recycled gas in the methanol blend to methane [12]. Also, the R_{Gibbs} model, based on Gibb's free energy minimization, was selected for the pre-modification equilibrium simulation for C_1 to C_4 hydrocarbons. Meanwhile, the R_{Gibbs} model was implemented for normal and modifying reactions as follows [17]:

$$SMR: H_2O + CH_4 \longleftrightarrow CO + 3H_2, \Delta H_{298K} = 206 \frac{kJ}{mol} \quad (1)$$

$$CDR: CO_2 + CH_4 \longleftrightarrow 2CO + 2H_2, \Delta H_{298K} = 247 \frac{kJ}{mol} \quad (2)$$

$$WGS: CO + H_2O \longleftrightarrow CO_2 + H_2, \Delta H_{298K} = -41 \frac{kJ}{mol} \quad (3)$$

$$CFR: CH_4 \longleftrightarrow C + 2H_2, \Delta H_{298K} = 75 \frac{kJ}{mol} \quad (4)$$

$$CFR: 2CO \longleftrightarrow C + CO_2, \Delta H_{298K} = -172 \frac{kJ}{mol} \quad (5)$$

The modifier operated five times at 500 ° C. In this example, because the reaction rate is high at high temperatures, reactions 1 to 3 were considered as a chemical equilibrium. To better simulate the modifier in the R_{Gibbs} model, a finite chemical equilibrium was considered. After modification, the synthesized gas was sent directly to the methanol compound reactor, without regulating the device. Because the synthesis gas coefficient is variable, the CO_2 correction was obtained by mixing with water vapor [16]. The CO_2 hydrogen conversion reactor in methanol was based on a copper catalyst that provided a good content of hydrogen. The methanol mixing reactor was operated at 250 ° C and 80 bar. The main reactions in the methanol compound reactor can be explained by the following three reactions [14]:

$$CO_2 + 3H_2 \longleftrightarrow CH_3OH + H_2O, \Delta H_{298K} = -49.5 \frac{kJ}{mol} \quad (6)$$

$$CO + 2H_2 \longleftrightarrow CH_3OH, \Delta H_{298K} = -90.5 \frac{kJ}{mol} \quad (7)$$

$$CO_2 + H_2 \longleftrightarrow CO + H_2O, \Delta H_{298K} = 41.2 \frac{kJ}{mol} \quad (8)$$

The methanol blending reactorwas simulated with the RPLUG reactor. However, the LHHW kinetic model was used to investigate the three primary reactions of methanol compounds [18]. The kinetic parameters in the LHHW model were obtained from previous experiments. The multipolar reactor had 11458 tubes, was 12 meters long, 0.03675 meters in diameter, and the particle density of the catalyst was 2000 kg/m^3 [19]. After mixing methanol with gas vapor, which contains unreacted gas, the methanol and nitrogen were removed from the top of the reactor. Meanwhile, the main crop of methanol and other products (water, DM, ethanol) was released from the bottom of the reactor. Part of the unreacted synthesized gas was recycled and returned to the methanol reformers to improve energy efficiency, such as CO_2 conversion [20]. The rest of the un-synthesized gas was ejected to avoid inert gas accumulation and used as a fuel to reduce NG consumption [21].

2.1 Exergy analysis

In the proposed cycle, greater use of thermal exergy and waste reduction in the plant are considered to increase efficiency [22]. As observed in Eq. (9), the complete cycle efficiency was obtained from the sum of the chemical and thermal efficiency of the system [23]. The electrical efficiency of the system was obtained from the product's thermal LHV used in the electrical performance using General Eq. (10) [24]. The overall performance of the system was calculated by Eq. (19) and is shown in Table 2.

$$\eta_{Total} = \eta_{electrical} + \eta_{heat} \quad (9)$$

$$\eta_{electrical} = \frac{W_{net}}{LHV_{fuel} * \xi_{fuel}} \quad (10)$$

Table 2. Exergy equations in cycle simulation [24].

Element	Exergy Efficiency	Equation
functional efficiency	$\eta_{Ex,f} = \frac{\sum Ex_{product}}{\sum Ex_{source}}$	11
Electrical efficiency	$\eta_{Ex,ele} = \frac{\sum Ex_{ele,out} - \sum Ex_{ele,in}}{\sum Ex_{fuel}}$	12
Exergy efficiency	$\eta_{Ex,total} = \frac{\sum Ex_{ele,out} + \sum Ex_{heat,out} - \sum P_{ele,in}}{\sum Ex_{fuel}}$	13
Exergy efficiency Fuel cell	$\eta_{Ex,f(cell)} = \frac{E_{ele}}{(Ex_{fuel,in} - Ex_{fuel,out}) + Ex_{ox,in} - E_{ox,out}}$	14
Exergy efficiency turbine	$\eta_{Ex,f(turbine)} = \frac{E_{shaft}}{Ex_{in} - \sum E_{out}}$	15
Exergy efficiency Steam reformer	$\eta_{Ex,f(reformer)} = \frac{Ex^{ch}_{productgas} - Ex^{ch}_{steam} - Ex^{ch}_{feed}}{(Ex^{tm}_{fluegas,in} - Ex^{tm}_{fluegas,out}) - (Ex^{tm}_{productgas} - Ex^{tm}_{steam} - Ex^{tm}_{feed})}$	16
Exergy efficiency heat exchanger	$\eta_{Ex,f(Heatexchanger)} = \frac{Ex_{p,out} - Ex_{p,in}}{Ex_{s,out} - Ex_{s,in}}$	17
Exergy efficiency drum	$\eta_{Ex,f(drum)} = \frac{Ex_{steam,out} - Ex_{steam,in}}{Ex_{evaporator,out} - Ex_{evaporator,in}}$	18
Exergy efficiency reactor	$\eta_{Ex,f(combustion\_chamber)} = \frac{Ex^{tm}_{flue\,gas} - Ex^{tm}_{fuel} - Ex^{tm}_{ox}}{Ex^{ch}_{fuel} + Ex^{ch}_{oc} - Ex^{ch}_{fluegas}}$	19
Exergy efficiency compressor, pump	$\eta_{Ex,f(Compressor,pump)} = \frac{Ex_{out} - Ex_{in}}{Ex_{shaft}}$	20

2.2 Exergoeconomics analysis

The method of external economic analysis is similar to environmental analysis [25]. This is an exergy analysis of the energy conversion system and then an economic analysis based on the Total Income Requirements (TRR) method that covers the entire life cycle of the energy conversion system. Initially, the total capital investment was calculated [24]. Then, based on the assumptions of economic, financial, operational, and market input parameters, the total annual revenue needed was calculated. This TRR shows the cost of producing the system products and offsets all costs incurred each year of the project's economic life to guarantee the industrial plant. After that, the annual variable costs of the product were related to the investment, operation, maintenance, fuel, and other costs (cost

categories) [26]. The equipment was converted into a series of equivalent annual payments. Then, by calculating the specific cost rate for each stream of matter and energy, costs were assigned to the respective exergy flows. Since the external economic analysis is well established, only the formulas of analogy with those used for the environmental analysis are presented in Table 3 [27].

Table 3. Equations for exergoeconomic and exergoenvironmental assessments [25, 26, 27].

Exergoeconomics		Exergoenvironmental	
Exergy stream cost rate	$C_j^{\cdot} = c_j * E_j^{\cdot}$	Exergoenvironmental :stream impact rate	$B_j^{\cdot} = b_j . E_j^{\cdot}$
Component cost balance	$\sum C^{\cdot} j,k,in + Z^{\cdot} k = \sum C^{\cdot} j,k,out$	Component environmental impact balance	$\sum B^{\cdot} j,k,in + Y^{\cdot} k = \sum B^{\cdot} j,k,out$
Component-related cost rate	$Z^{\cdot} k = Z_k^{CL} + Z_k^{OM}$	Component-related environmental impact rate	$Y_k = Y_K^{CL} + Y_K^{OM} + Y_K^{DI}$
The component relative cost difference	$r_k = \frac{C_{P,k} + C_{F,k}}{C_{F,k}}$	Component relative environmental impact difference	$r_{b,k} = \frac{b_{P,k} - b_{F,k}}{b_{F,k}}$
Component exergoeconomic factor	$f_k = \frac{Z_k}{Z_k + C_{D,k}}$	Component exergoenvironmental factor	$f_{b,k} = \frac{Y_k}{Y_k + B_{D,k}}$

2.3 Exergoenvironmental analysis

As mentioned earlier, all previously developed thermodynamic approaches to allocation are useful for formulating the complexity in energy systems with several desirable ones. Energy products in these efforts have responded to problems related to micro-level allocation to access detailed process information that the current economy has failed to do [28]. More precisely, this inaccuracy stems from neglecting the process details and aggregating the entire process of each subsystem. This accumulation results in a different allocation share among the products in the use of P-type auxiliary equations. However, there are accounting constraints that are used for the macro level [29]. There are several non-energy products in the same unit (along with energy goods) that cannot be evaluated based on their sensitivity such as petrochemical and fresh products. Water, is at least the second top assessment of responsibilities in the absence of a better assessment method. Modification of the auxiliary equations in the standard environmental approach is proposed to rationally allocate the standard level of greenhouse gas emissions among producers, while the original equilibrium equations remain the same [30].

The idea of this research is to replace the high costs with the exergy content in the P/F auxiliary equations between energy and non-energy flows, and if all flows for which environmental load is assigned are energy flows, P/F rules will be applied [31]. (Sums up for each subsystem). If all the streams for which the environmental load is assigned are non-energy streams, the exergy content P/F rules should be replaced with additional costs. This is because the high cost reflects the amount of exergy consumed in the production of materials, and may, therefore, represent exergy destruction and greenhouse gas emissions. These high costs are available in many previous studies, e.g., [31, 32], or can also be calculated directly by the exergy consumption concentration (CEXC) approach. For simplicity, the high cost from the literature are used in this study. In other words, if the units have both energy and non-energy flows, this allocation is based on the classical commodity method, which assumes that the

environmental impact is due to significant products from foreign and other sources[32]. Greenhouse gas emissions are allocated according to one of the two rules mentioned above. The contribution of each unit to the greenhouse gas emissions was calculated using the environmental specific load, which is calculated in the exergy unit of each stream. This was done using the Bastianoni carbon emission enhancement (CEA) approach presented in [15, 33]. In this method, presented as average upstream and downstream debt allocation methods, the cumulative environmental loads per unit of production are summarized, and the percentages of aggregates represent the environmental responsibility of the resultant unit [32]. The thermodynamic methods for distributing the load across the outputs are useful concepts for formulating complex energy systems with several desired energy products. These approaches allow for the identification of problems related to the transfer of load at the micro-level, conventional economic theories are often too complicated at this level. However, due to the lack of process details and the integration of the whole process of each subsystem, it is less accurate than the macro-level analysis [33]. This combination creates a different allocation of stocks between stocks. Table 4 summarizes the rules listed below:

Table 4. The method used in different cases [33, 34].

Case	Specification	Allocation Rule	Formulation
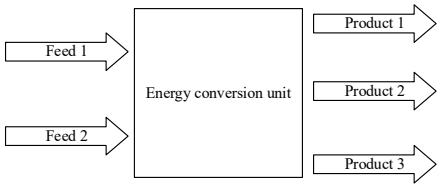	Energy carriers e.g., Cogeneration unit	P-type/F-type	$b_1 = b_2 = b_3$
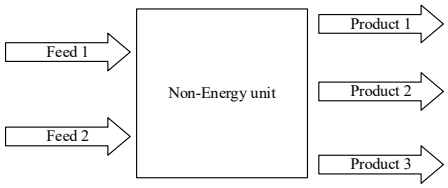	Non-energy carriers e.g. Ammoniac and Ammonia plants	P-type/F-type replacing exergetic costs instead of exergies	$\frac{b_1E_1}{CEXC_1} = \frac{b_2E_2}{CEXC_2} = \frac{b_3E_3}{CEXC_3}$
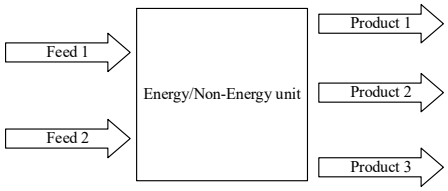	P1 and P2: Energy carriers P3: Non-energy carrier e.g., crude oil distillation column	5th principle suggested by Finnveden subtracting P3 and Conventional exergoenvironment al P-type/ F-type	$b_1 = b_2$ $\frac{b_3E_3}{CEXC_3} = cte$
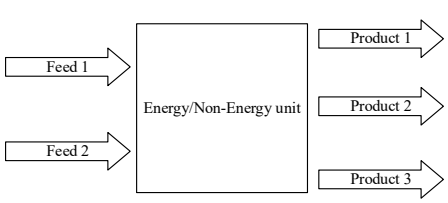	P1, P2: NonEnergy carriers P3: Energy carrier e.g., Cement production with waste heat recovery power plant	5th principle suggested by Finnveden subtracting P3 and Conventional exergoenvironment al P-type/ F-type replacing exergetic costs instead of exergies	$b_3 = cte$ $\frac{b_1E_1}{CEXC_1} = \frac{b_2E_2}{CEXC_2}$

It may be possible to calculate the contribution of each unit to the emission of environmental gases using the specific environmental charge calculated in the exergy unit of each stream, (b). This is done using the Bastianoni carbon emission enhancement (CEA) approach presented in [34]. In this method, presented as the average upstream and downstream debt allocation methods, the accumulated environmental loads per unit of production are normalized. "The appropriate level of aggregation identifies the

behavior of each process unit and its purpose in the overall production process [31]. Again, it is worth noting that as the analytical level of analysis increases, the accuracy of the results decreases. Products are considered as units of minimum scale, so it is advisable to go into the details of the process as far as data is available or time-limited analysisallows[35].

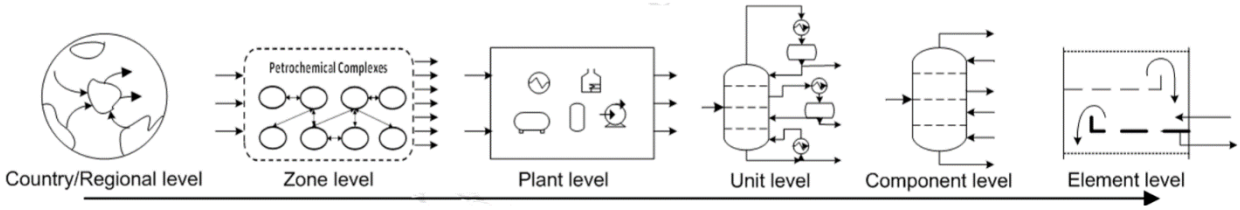

Figure 2. Different levels of system analysis [35].

A more comprehensive view requires more data to perform a more time-consuming analysis. However, more complexities are considered and more accurate results are obtained [36]. The accumulation error sequence depends on the amount of accumulation and file size. The previously developed thermodynamics-based methods described in Section 2.1 are used for component surface analysis but are limited to a specific unit of energy (and, in some cases, the plant surface) as a specific application. Such limited logic may not apply to environmental accounts in cases where an area is affected by manufacturing activities in the macro analysis of the current work system, as recommended in the literature [33], due to a large number of plants, The lack of information and the extent of the area of interest for environmental analysis is the study of the area concerned. Addressed. It placed. In further studies on the type of policy, this method may also be applied at the regional or country level, while reducing the level of accuracy [34]. However, in some cases, the accumulation error may be significant as some manufacturing processes consume small amounts of pollutants (such as renewable energy), nutrients, or even contaminants produced elsewhere. Use as raw materials (such as carbonated drinking process) Alternatively, treatment units) In such cases, the use of type P fraud is deceptive [34]. Therefore, the choice of aggregate level in the analysis and the category of environmental impacts in the analysis should be considered.

Another challenge in using high costs is the error in importing secondary energy carriers as fuel. In such cases, if environmental loads (outside of local pollution management) are not taken outside the boundaries of the system, the destruction of exergy products will result in high costs of imported fuel [35]. However, economically and flexibly, the intermediate feed is usually processed near the end consumer. In such cases, it is recommended to extend the boundaries of the system to consider all the environmental impacts of the production activity under study. Otherwise, if emissions do not affect the purpose and environment of the area, it is advisable to reduce the share of high out-of-system costs by importing secondary energy carriers or processed feeds [36]. However, because of all the shortcomings, the idea of replacing the exergy contents with the exergy destruction/high costs in the allocation process, the notion of a share in the propagation related to the exergy destruction/additional costs, makes the managers' thermodynamic logic. Environmental decisions are more acceptable to producers, and it also extends the use of proprietary thermodyna m ic methods to a broader range of energy or n on-energy systems [21, 36]. The performance p a rameters of this plant can be described using the following indexes in Table 5 [37].

Table 5. The performance factors of the NDCL plant [31-36].

Factor	Formula
The Energy performance plant	$\eta_{Gross} = \frac{W_{gross}}{m_{fuel} * LHV_{fuel}} * 100$
methanol efficiency	$\eta_{methanol} = \frac{LHV_{H_2}.m_{methanol}}{m_{fuel} * LHV_{fuel}} * 100$
Carbon capture efficiency	$\eta_{co_2} = \frac{CO_{2,i} - CO_{2,o}}{CO_{2,i}}$
specific carbon dioxide emission	$E_{co_2} = \frac{m_{co_{2emit}}}{W_{net}}$
the annual CO_2 emissions rate	$\varepsilon_{fCO_2} = \frac{m_{CO_{2emit}}}{3.6 * E_{chf}}$
The exergy efficiency of the plant	$ExE = \frac{\xi_{H_2}.LHV_{H_2}.m_{H_2} + \xi_{FA}.LHV_{FA}.m_{FA}}{Electricity\ consumption}$

3. Results and discussion

We conducted a study of different samples under operating conditions, as shown in standard Tables of S2 to S4 from SI [38]. During the study, the CGTM process was evaluated with seven different recovery coefficients to investigate its effect on the CO_2/(CO + CO_2) ratio in the synthesized gas as well as all CO_2 conversions and energy efficiency. The molar ratio of the fresh feed CO_2/NG/H_2O was stabilized over a range of (0.3-0.5):1:(1.5-2.5) to keep the process away from the sediment area. Also, the operating conditions have been chosen to avoid carbon compounds. The synthesized gas reformer was manufactured with changeable compounds, and the optimal H_2/(2CO+3CO_2) ratio in the synthesis gas for the methanol blend with the copper catalyst should be in the range of 0.99 to 1.1 (Table S2 to S4). The molar shift of the input feed was achieved by placing it in a reasonable area. The ratio of H_2/(2CO+3CO_2) in the gas synthesis varied with the recovery coefficient. We thus fixed the optimal H_2/(2CO + 3CO_2) ratio in the gas synthesis, and the CO_2/NG ratio should be adjusted based on Tables S2 to S4 [38]. As shown in Figure 3(a), the CO_2/(CO + CO_2) ratio in the gas can be increased by increasing the recovery coefficient. The reason for this can be explained by the more significant amount of conversion of CO from CO_2 to methanol in the methanol system. This increases with the recovery coefficient of the amount of CO_2 accumulated in the gas that feeds the inlet of the methanol compound reactor. However, it is noteworthy that the increased recovery factor as opposed to the accumulation of CO_2 in the synthesis gas. As a result, the total amount of CO_2 emitted from the input process is improved, and the total amount of CO_2 converted decreased, as shown in Figure 3b.

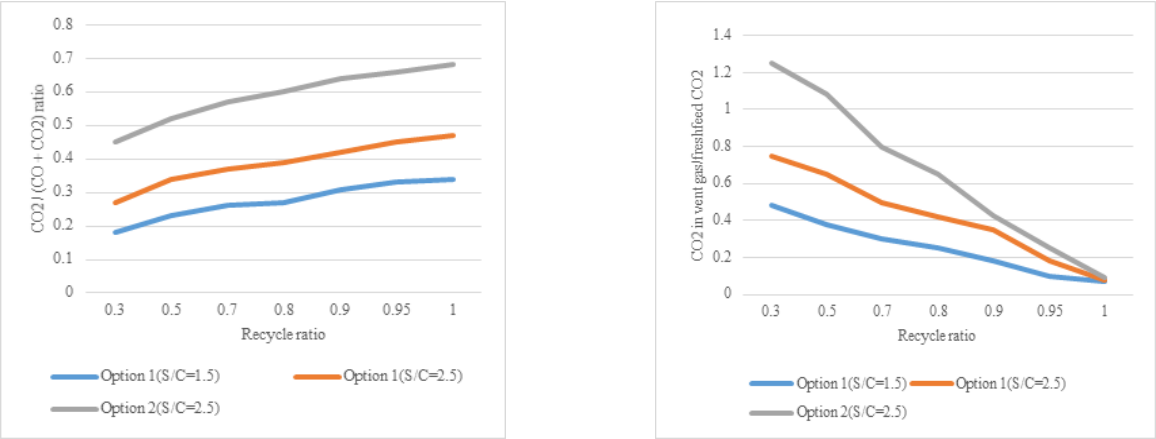

Figure 3. (a) Influence of recovery ratio on the CO_2 / ($CO + CO_2$) ratio of the synthesized gas. (b) Impact of recycling ratio on total CO_2 conversion.

In the second option (Option 2), the CO_2 / ($CO + CO_2$) ratio increases when the recycle ratio value is approximately 0.55. The total amount of CO_2 conversion is close to zero. Also, when the coefficient of recovery is increased to about 0.98, nearly 95% of the CO_2 in both choices is converted. The conversion of hydrogen to CO_2, as well as its modification, can be attributed to the methanol and correction system, respectively. In the methanol compound reactor, a high $CO_2/(CO+CO_2)$ ratio with the optimal $H_2/(2CO+3CO_2)$ ratio modifies the conversion of CO_2 to methanol by CO_2 hydrogen conversion. A higher the $CO_2/(CO+CO_2)$ ratio, meanwhile, results in higher passages and final CO_2 conversion. Moreover, the recovered CO_2 in the rectifier is also converted by the modified CO_2. Meanwhile, in the processes mentioned earlier, the recycled CO_2, which is sent to methanol reformers, is converted into methanol and gas synthesis. As such, a significant amount of CO_2 gas is reduced by recycling.

Methanol production is increased by increasing the recovery coefficient [38]. More methanol can be produced by the unreacted synthetic gas due to the incoming fresh feed, and the flow rate at the modifier output as well as the input of the methanol compound reactor increases as the recovery coefficient increases. The reason for this can be attributed to the increased volume of recycled synthesis gas [38], if the recovery coefficient is increased, then technically methanol production can be improved, increasing energy efficiency and reducing CO_2 emissions. Economically, one can also see an increase in current interest. The size of the two reactors should be increased because the spatial velocity for all samples is assumed to be the same. This can significantly increase operating costs and initial capital. In both economic and technical terms, the recovery coefficient should be determined according to the defined conditions to maximize the economic benefit.

Furthermore, two essential energy yields, called T_{eff} heat efficiency and C_{eff} carbon efficiency, must be considered in the information. In a caustic modifier, NG is commonly used as a gas fuel. However, to increase energy efficiency, the discharged gas is used as a burner force to reduce NG consumption. T_{eff} and C_{eff} can also be increased. In some instances in the present study (usually when the recovery coefficient of choice 2 (Option 2) is less than 0.7 and in choice 1 (Option1) less than 0.5), heat energy is required for the modifier to be able to fully absorb the gases. Burn the extraneous extrusion. In other instances, however, the thermal energy generated by the additional gases for the modifier is not beneficial, especially when the recovery coefficient is increased, i.e., when the recovery coeffiicient exceeds 0.7 for Option 1 and 0.8 for Option 2. In other words, extra NG gas is needed at high recycling rates. T_{eff} and C_{eff} are calculated in two different ways under the conditions we mentioned. Here are some specific methods for calculating C_{eff} and T_{eff}.

If the LHV of excess gases exceeds the value of the heat capacity [24, 33, 37]:

$$T_{eff} = \frac{\text{LHV of methanol}}{\text{LHV of feed NG}} \quad (21)$$

$$C_{eff} = \frac{\text{total moles of C atoms in methanol}}{\text{total moles of C atoms in feed NG}} \quad (22)$$

If the LHV of the additional gases is less than the value of the original heat capacity:

$$T_{eff} = \frac{\text{LHV of methanol}}{\text{LHV of feed NG} \times \text{heat duty} = 0.8 \_ \text{LHV of vent gas}} \quad (23)$$

$$C_{eff} = \frac{\text{total moles of C atoms in methanol}}{\text{total moles of C atoms in feed NG} \times \text{total moles of C atoms in fuel NG}} \quad (24)$$

When the total mole of carbon atoms in the NG is refreshed:

$$\text{total moles of C atoms in fuel NG} = \frac{\text{heat duty} = 0.8 \_ \text{LHV of vent gas} \times 1.012}{\text{LHV of fuel NG}} \quad (25)$$

In Equations 23 and 24, the value of 0.8 is estimated for the transient thermal efficiency of the modifier and is considered as the thermal duty of the entire thermal apparatus, such as modifiers and heaters in the modifier.

The number 1.012 in Equation 25 indicates the mole value of each carbon atom relative to the mole value of NG fuel used in the present studies.

Figure 4 shows the T_{eff} and C_{eff} values for both choices in different recovery coefficients. Both values increased steadily as the recovery coefficient increased. This result was found even in the region where the recovery coefficient was high (between 0.8 and 0.98)in the GTL process that uses an iron catalyst and F-T compound unit. However, this differs from the GTL process which uses a cobalt catalyst and F-T blend machine, which performs at high recovery rates. The increase in energy efficiency here is mainly due to the increase in CO_2 conversion with a high recycling coefficient in the methanol mixing reactor. As the recovery coefficient increases, more CO_2 is converted to methanol in the CO_2 reactor. T_{eff} and C_{eff} thus increase with an increasing recycling factor. However, only a small amount of CO_2 conversion is accomplished by the WGS reaction in the GTL process with the F-T combination reactor and cobalt catalyst.

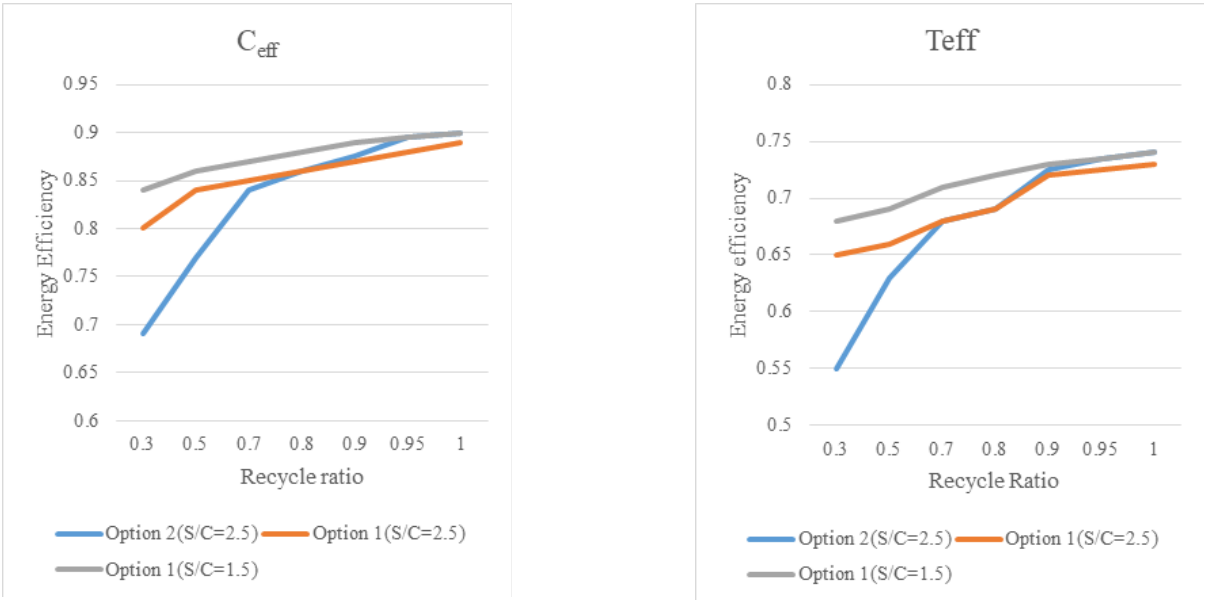

Figure 4. Impact of recovery ratio on energy efficiency: (a) C_{eff} and (b) T_{eff}.

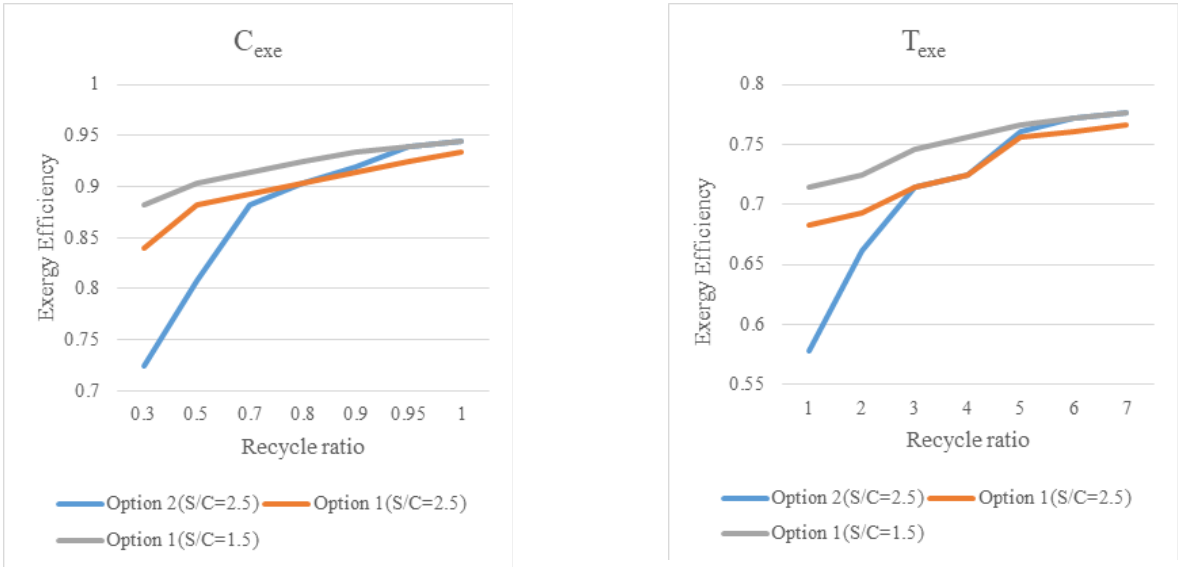

Figure 4. Impact of Recovery Ratio on Exergy Efficiency: (a) C_{exe} and (b) T_{exe}.

Figure 5 depicts T_{eff} and C_{eff} for both fission choices. Although T_{eff} and C_{eff} tend to move downward with a decreasing gap coefficient, no significant change is seen with a fission coefficient change. T_{eff} and C_{eff} have their highest values when the refractive index drops to zero. Since the CDR reaction is very endothermic, more CO_2 must be sent to the modifier, and this requires more required energy. Although excess synthesis gas is produced concurrently with the increase in the fission coefficient, it seems that the heat duty co-operation is dominated by T_{eff} and C_{eff}. As the fission coefficient increases, according to observations, it seems that the fission coefficient will have lower energy efficiency in CGTM.

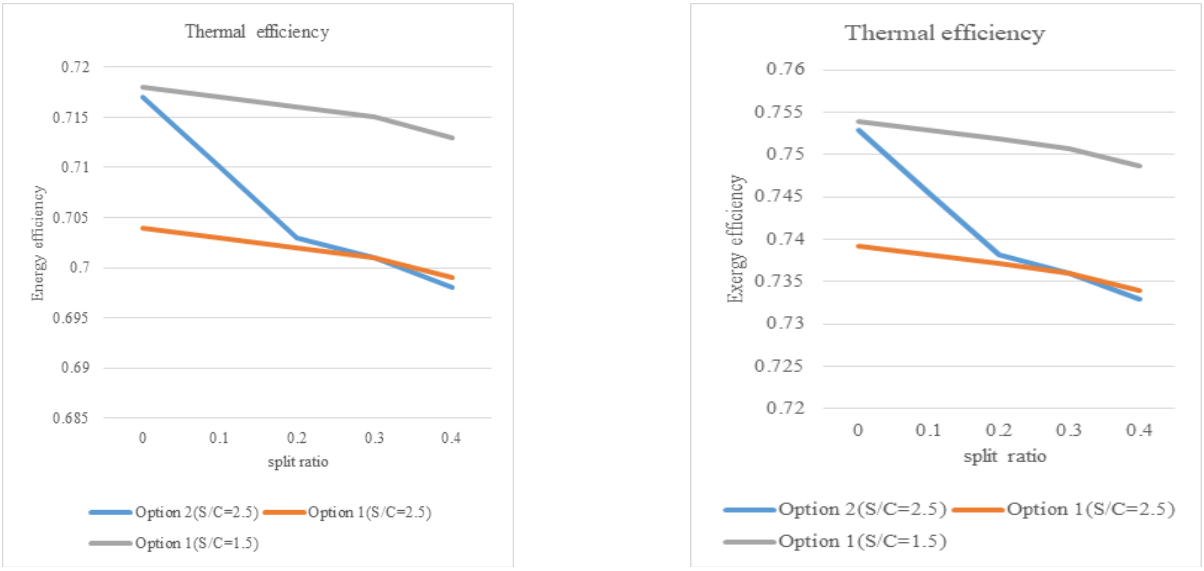

Figure 5. Impact of split ratio on efficiency: (a) energy efficiency and (b) exergy efficiency.

As mentioned earlier, CO_2 is converted to methanol by the CDR reaction plus hydrogen conversion in the modifier and reactor, respectively. Overall, the equilibrium conversion of CO_2 by the CDR reaction in the modifier is higher than the conversion of CO_2 to hydrogen in the methanol-combined reactor with copper catalyst. Particularly under the application of the low recycling factor used in modern studies. It should, therefore, be noted that CO_2 conversion by CO_2 hydrogen conversion can improve the recovery coefficient.

As can be seen in Figure 2, the ratio of CO_2/(CO +

CO_2) in the first choice under the same conditions is always lower than the second choice, due to the different structure of the two processes. This is in agreement with the results in [38]. In Option 1, fresh CO_2 is converted to CO by the CDR reaction of the modifier, resulting in a decrease in CO_2 in the synthesis gas content. However, in Option 2, fresh CO_2 is directly fed to the methanol mixing reactor without consuming CO_2 in the modifier. In option 1, the $CO_2/(CO + CO_2)$ vapor-to-carbon ratio (S/C=1.5) is lower than that for (S/C=2.5). The reason for this is the competition between CDR and SMR reactions in the breeder. These issues indicate that a lower S/C ratio improves the CO_2 conversion rate and leads to a lower $CO_2/(CO + CO_2)$ ratio. As shown in Figure 3, the amount of CO_2 in the exhaust gas for Option 1 is lower than Option 2. We can conclude that CO_2 consumption by the CDR process is much higher than the CO_2 hydrogenation process under the same conditions. However, Option 1 with the S/C=1 ratio shows less CO_2 in the exhaust gas, which can improve CO_2 conversion at a low S/C ratio. Conversely, the difference in the amount of CO_2 in the exhaust gas between Option 1 and 2 decreases with increasing recovery coefficient. This happens for Option 2 by increasing the CO_2 conversion in the methanol reactor with a higher $CO_2/(CO+CO_2)$ ratio. In addition, as we can see in Fig. 4, the T_{eff} and C_{eff} calculated for Option 1 are greater than Option 2 with a S/C=2.5. When the coefficient of recovery is between 0.3 and 0.8, the results are quite the opposite to those obtained. Higher T_{eff} and C_{eff} values for Option 1 with a S/C=2.5 ratio and low recovery coefficient (between 0.3 to 0.8) are mainly due to the greater conversion of CO_2 into the modifier by the CDR reaction, and the heat generated by the exhaust gases. The power supply needed by the device is improved. In contrast, higher T_{eff} and C_{eff} values for Option 2 with a high recovery coefficient (between 0.8 to 0.98) generally lead to greater conversion of CO_2 into the methanol mixing reactor as well as lower energy consumption in the rectifier when greater NG is required and attributed. Besides, Option 1 with the S/C ratio = 1.5 indicates that higher energy efficiency occurs with a lower S/C ratio. However, with high recovery coefficients, Option 2's the S/C=2.5 ratio is comparable to Option 1's S/C = 1.5 ratio, this is due to the increased CO2 conversion in the methanol mixing reactor and the reduction in energy consumption in the correction plant. As shown in Fig. 5, T_{eff} and C_{eff} were slightly lower in Option 1 with an S/C = 2.5 ratio than for Option 2 with a lower fission coefficient, this may be due to the greater CO_2 conversion in the combined reactor in Option 1 and the methanol and consumption of less energy in the rectifier in Option 2. Examination of CO_2 emissions, such as T_{eff} and C_{eff} for Options 1 and 2 at S/C=2.5 leads us to conclude that Option 2 has more problems in the CGTM process, especially with high recovery coefficients, as shown in Figure 6. The total amount of CO_2 emitted in the CGTM process is much lower than the original GTM with identical fission and recovery coefficients.

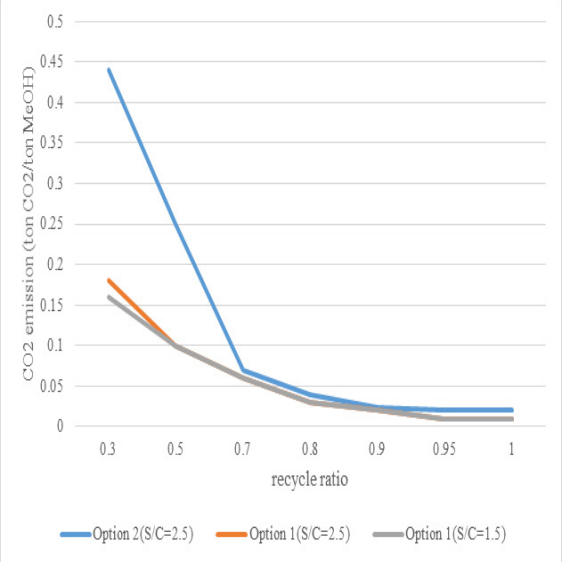

Figure 6. Impact of recycling ratio on total CO_2 emissions.

Table 6 compares the performance results of CGTMs and GTMs. For the CGTM process, the recycling coefficients increased from 7.0 to 95.0, C_{eff} from 5 to 3.8%, T_{eff} from 8.4 to 9.7%, and methanol production from 4.17 to 1.47% as compared to the original GTM.

Table 6. The results of different options and assumptions.

exergy destruc-tion cost ($/s)	F(%)	r(%)	Cexe	Texe	MSR	Re-former (kmol/h)	Ceff.	Teff.	MeOH	NG (kmol/h)	H2O (kmol/h)	CO2 (kmol/h)	R2C	R1b	S2	R1	S/C ratio	Op.
1722.643	72.46368	34.67454	0.93765	0.7539	858.2154	366.5788	0.87514	0.70364	122.0394	98	155.82	42.14	0.9849	0.3283	0.1	0.95	1.5	**1**
1744.127	71.57107	34.24741	0.9261	0.74445	1015.182	483.4928	0.86436	0.69482	121.1672	98	247.94	44.1	0.98882	0.47726	0.1	0.95	2.5	**1**
1728.449	72.22024	34.55805	0.9345	0.7518	1249.696	460.1982	0.8722	0.70168	118.139	98	247.94	41.65	0.99372	0.63014	0.1	0.95	2.5	**2**
1758.08	71.00305	33.97561	0.91875	0.74025	613.1664	343.1568	0.8575	0.6909	101.9004	98	155.82	36.26	0.98784	0.24206	0.1	0.7	1.5	**1**
1797.103	69.46127	33.23785	0.8988	0.7245	691.733	455.5138	0.83888	0.6762	98.0392	98	247.94	39.2	0.97706	0.38514	0.1	0.7	2.5	**1**
1807.662	69.05554	33.04371	0.89355	0.72135	799.9544	427.8974	0.83398	0.67326	88.4744	98	247.94	37.24	0.99078	0.55174	0.1	0.7	2.5	**2**
1876	66.5472	31.872	0.861	0.6951	763.6258	427.8582	0.8036	0.64876	81.8692	98	247.94	0	2.05702	0.31654	0.1	0.7	2.5	**Base case**

R = recycle / (recycle + vent) (= R recycling / (recycling + suction)), (2) S = recycle-to-reformer / recycle (S = optimal recycling / recycling)

R1 = CO_2 / (CO_2 + CO)

R2 = H_2 / (2CO + 3CO_2) c, where R1 and R2 refer to the composition of the synthesis gas at the inlet of the methanol synthesis unit.

4. Conclusion

We have proposed two CGTM methods with different fresh CO_2 feed points for the beneficial use of CO_2. We investigated the effect of the refractive index and recovery coefficient on heat and carbon efficiency as well as the overall CO_2 conversion rate in both proposed CGTMs. In addition, we compared the performance of both CGTMs with the original GTMs. As can be seen from the simulation results, the carbon and heat efficiency are sensitive to the recycling factor, and a higher recycling factor appears to improve CO_2 conversion, increase carbon and heat efficiency, and reduce emissions [39]. However, the fission factor appears to have little effect on the thermal and carbon efficiency and does not affect the optimized recycling of the corrective device. Compared to the initial GTM process, the thermal and carbon efficiency for both CGTMs has been successfully increased, and the CO_2 emissions significantly reduced due to the optimal use of CO_2 in methanol for each modifier. Exergy efficiency, environmental indicators, and exergy degradation costs were also significantly improved during this process [40].

References

[1] Sunghoon Kim, Jiyong Kim, The optimal carbon and hydrogen balance for methanol production from coke oven gas and Linz-Donawitz gas: Process development and techno-economic analysis, Fuel, Volume 266, 2020,117093, ISSN 0016-2361, https://doi.org/10.1016/j.fuel.2020.117093.

[2] Leon G.A. van de Water, Sam K. Wilkinson, Richard A.P. Smith, Michael J. Watson, Understanding methanol synthesis from CO/H2 feeds over Cu/CeO2 catalysts, Journal of Catalysis, Volume 364, 2018, Pages 57-68, ISSN 0021-9517,https://doi.org/10.1016/j.jcat.2018.04.026.

[3] Peipei Zhang, Yuya Araki, Xiaobo Feng, Hangjie Li, Yuan Fang, Fei Chen, Lei Shi, Xiaobo Peng, Yoshiharu Yoneyama, Guohui Yang, Noritatsu Tsubaki, Urea-derived Cu/ZnO catalyst being dried by supercritical CO2 for low-temperature methanol synthesis, Fuel, Volume 268, 2020, 117213, ISSN 0016-2361, https://doi.org/10.1016/j.fuel.2020.117213.

[4] Sasinun Thirabunjongcharoen, Palang Bumroongsakulsawat, Piyasan Praserthdam, Sumittra Charojrochkul, Suttichai Assabumrungrat, Pattaraporn Kim-Lohsoontorn, Thermally double coupled reactor coupling aqueous phase glycerol reforming and methanol synthesis, Catalysis Today, 2020, ISSN 0920-5861, https://doi.org/10.1016/j.cattod.2020.03.043.

[5] Giacomo Butera, Rasmus Østergaard Gadsbøll, Giulia Ravenni, Jesper Ahrenfeldt, Ulrik Birk Henriksen, Lasse Røngaard Clausen, Thermodynamic analysis of methanol synthesis combining straw gasification and electrolysis via the low temperature circulating fluid bed gasifier and a char bed gas cleaning unit, Energy, 2020, 117405, ISSN 0360-5442, https://doi.org/10.1016/j.energy.2020.117405.

[6] Karittha Im-orb, Amornchai Arpornwichanop, Process and sustainability analyses of the integrated biomass pyrolysis, gasification, and methanol synthesis process for methanol production, Energy, Volume 193, 2020, 116788, ISSN 0360-5442, https://doi.org/10.1016/j.energy.2019.116788.

[7] Woo Jin Lee, Ankur Bordoloi, Jim Patel, Tejas Bhatelia, The effect of metal additives in Cu/Zn/Al2O3 as a catalyst for low-pressure methanol synthesis in an oil-cooled annulus reactor, Catalysis Today, Volume 343, 2020, Pages 183-190, ISSN 0920-5861, https://doi.org/10.1016/j.cattod.2019.03.041.

[8] Usama Ahmed, Techno-economic feasibility of methanol synthesis using dual fuel system in a parallel process design configuration with control on green house gas emissions, International Journal of Hydrogen Energy, Volume 45, Issue 11, 2020, Pages 6278-6290,ISSN 0360-3199, https://doi.org/10.1016/j.ijhydene.2019.12.169.

[9] Melis S. Duyar, Alessandro Gallo, Jonathan L.

Snider, Thomas F. Jaramillo, Low-pressure methanol synthesis from CO2 over metal-promoted Ni-Ga intermetallic catalysts, Journal of CO2 Utilization, Volume 39, 2020, 101151, ISSN 2212-9820, https://doi.org/10.1016/j.jcou.2020.03.001.

[10] Shoujie Ren, Xiao Fan, Zeyu Shang, Weston R. Shoemaker, Lu Ma, Tianpin Wu, Shiguang Li, Naomi B. Klinghoffer, Miao Yu, Xinhua Liang, Enhanced catalytic performance of Zr modified CuO/ZnO/Al2O3 catalyst for methanol and DME synthesis via CO2 hydrogenation, Journal of CO2 Utilization, Volume 36, 2020, Pages 82-95, ISSN 2212-9820, https://doi.org/10.1016/j.jcou.2019.11.013.

[11] Dominik Schack, Georg Liesche, Kai Sundmacher, The FluxMax approach: Simultaneous flux optimization and heat integration by discretization of thermodynamic state space illustrated on methanol synthesis process, Chemical Engineering Science, Volume 215, 2020, 115382, ISSN 0009-2509, https://doi.org/10.1016/j.ces.2019.115382.

[12] Wanqi Liu, Dunyou Wang, Junfeng Ren, Methanol synthesis from CO2/H2 on Cu (1 0 0): Two-tier ab initio molecular dynamics study, Applied Surface Science, Volume 505, 2020, 144528, ISSN 0169-4332, https://doi.org/10.1016/j.apsusc.2019.144528.

[13] Tapio Salmi, Kari Eränen, Pasi Tolvanen, J.-P. Mikkola, Vincenzo Russo, Determination of kinetics and equilibria of heterogeneously catalyzed gas-phase reactions in gradientless autoclave reactors by using the total pressure method: Methanol synthesis, Chemical Engineering Science, Volume 215, 2020, 115393, ISSN 0009-2509, https://doi.org/10.1016/j.ces.2019.115393.

[14] Humberto Blanco, Stevie Hallen Lima, Victor de Oliveira Rodrigues, Luz Amparo Palacio, Arnaldo da Costa Faro Jr., Copper-manganese catalysts with high activity for methanol synthesis, Applied Catalysis A: General, Volume 579, 2019, Pages 65-74, ISSN 0926-860X, https://doi.org/10.1016/j.apcata.2019.04.021.

[15] Shashwata Ghosh, Srinivas Seethamraju, Feasibility of reactive distillation for methanol synthesis, Chemical Engineering and Processing - Process Intensification, Volume 145, 2019, 107673, ISSN 0255-2701, https://doi.org/10.1016/j.cep.2019.107673.

[16] Anthony R. Richard, Maohong Fan, Rare earth elements: Properties and applications to methanol synthesis catalysis via hydrogenation of carbon oxides, Journal of Rare Earths, Volume 36, Issue 11, 2018, Pages 1127-1135, ISSN 1002-0721, https://doi.org/10.1016/j.jre.2018.02.012.

[17] Ben Redondo, Milinkumar T. Shah, Vishnu K. Pareek, Ranjeet P. Utikar, Paul A. Webley, Jim Patel, Woo Jin Lee, Tejas Bhatelia, Intensified isothermal reactor for methanol synthesis, Chemical Engineering and Processing - Process Intensification, Volume 143, 2019, 107606, ISSN 0255-2701, https://doi.org/10.1016/j.cep.2019.107606.

[18] Seyed Sina Hosseini, Mehdi Mehrpooya, Ali Sulaiman Alsagri, Abdulrahman A. Alrobaian, Introducing, evaluation and exergetic performance assessment of a novel hybrid system composed of MCFC, methanol synthesis process, and a combined power cycle, Energy Conversion and Management, Volume 197, 2019, 111878, ISSN 0196-8904, https://doi.org/10.1016/j.enconman.2019.111878.Klara Wiese, Ali M. Abdel-Mageed, Alexander Klyushin, R. Jürgen Behm, Dynamic changes of Au/ZnO catalysts during methanol synthesis: A model study by temporal analysis of products (TAP) and Zn LIII near Edge X-Ray absorption spectroscopy, Catalysis Today, Volume 336, 2019, Pages 193-202, ISSN 0920-5861, https://doi.org/10.1016/j.cattod.2018.11.074.

[19] Imran Abbas, Honggon Kim, Chae-Ho Shin, Sungho Yoon, Kwang-Deog Jung, Differences in bifunctionality of ZnO and ZrO2 in Cu/ZnO/ZrO2/Al2O3 catalysts in hydrogenation of carbon oxides for methanol synthesis, Applied Catalysis B: Environmental, Volume 258, 2019, 117971, ISSN 0926-3373, https://doi.org/10.1016/j.apcatb.2019.117971.

[20] R. Guil-López, N. Mota, J. Llorente, E. Millán, B. Pawelec, R. García, R.M. Navarro, J.L.G. Fierro, Data on TGA of precursors and SEM of reduced Cu/ZnO catalysts co-modified with aluminium and gallium for methanol

synthesis, Data in Brief, Volume 24, 2019, 104010, ISSN 2352-3409, https://doi.org/10.1016/j.dib.2019.104010.

[21] Markus Kaiser, Hannsjörg Freund, A multimodular pseudoheterogeneous model framework for optimal design of catalytic reactors exemplified by methanol synthesis, Chemical Engineering Science, Volume 206, 2019, Pages 401-423, ISSN 0009-2509, https://doi.org/10.1016/j.ces.2019.04.036.

[22] S. Likhittaphon, R. Panyadee, W. Fakyam, S. Charojrochkul, T. Sornchamni, N. Laosiripojana, S. Assabumrungrat, P. Kim-Lohsoontorn, Effect of CuO/ZnO catalyst preparation condition on alcohol-assisted methanol synthesis from carbon dioxide and hydrogen, International Journal of Hydrogen Energy, Volume 44, Issue 37, 2019, Pages 20782-20791, ISSN 0360-3199, https://doi.org/10.1016/j.ijhydene.2018.07.021.

[23] Minji Son, Yesol Woo, Geunjae Kwak, Yun-Jo Lee, Myung-June Park, CFD modeling of a compact reactor for methanol synthesis: Maximizing productivity with increased thermal controllability, International Journal of Heat and Mass Transfer, Volume 145, 2019, 118776, ISSN 0017-9310, https://doi.org/10.1016/j.ijheatmasstransfer.2019.118776.

[24] H. A. Ozgoli, H. Ghadamian, R. Roshandel & M. Moghadasi (2015) Alternative Biomass Fuels Consideration Exergy and Power Analysis for Hybrid System Includes PSOFC and GT Integration, Energy Sources, Part A: Recovery, Utilization, and Environmental Effects, 37:18, 1962-1970, DOI: 10.1080/15567036.2012.654898

[25] Khunnawat Ountaksinkul, Paravee Vas-Umnuay, Nattapong Kasempremchit, Palang Bumroongsakulsawat, Pattaraporn Kim-Lohsoontorn, Tara Jiwanuruk, Suttichai Assabumrungrat, Performance comparison of different membrane reactors for combined methanol synthesis and biogas upgrading, Chemical Engineering and Processing - Process Intensification, Volume 136, 2019, Pages 191-200, ISSN 0255-2701, https://doi.org/10.1016/j.cep.2019.01.009.

[26] Humberto Blanco, Stevie Hallen Lima, Victor de Oliveira Rodrigues, Luz Amparo Palacio, Arnaldo da Costa Faro Jr., Copper-manganese catalysts with high activity for methanol synthesis, Applied Catalysis A: General, Volume 579, 2019, Pages 65-74, ISSN 0926-860X, https://doi.org/10.1016/j.apcata.2019.04.021.

[27] Guo Wang, Dongsen Mao, Xiaoming Guo, Jun Yu, Methanol synthesis from CO2 hydrogenation over CuO-ZnO-ZrO2-MxOy catalysts (M=Cr, Mo and W), International Journal of Hydrogen Energy, Volume 44, Issue 8, 2019, Pages 4197-4207, ISSN 0360-3199, https://doi.org/10.1016/j.ijhydene.2018.12.131.

[28] Babusi Balopi, Paul Agachi, Danha, Methanol Synthesis Chemistry and Process Engineering Aspects-A Review with Consequence to Botswana Chemical Industries, Procedia Manufacturing, Volume 35, 2019, Pages 367-376, ISSN 2351-9789, https://doi.org/10.1016/j.promfg.2019.05.054.

[29] A. Mirvakili, S. Chahibakhsh, M. Ebrahimzadeh-sarvestani, E. Soroush, M.R. Rahimpour, Modeling and assessment of novel configurations to enhance methanol production in industrial mega-methanol synthesis plant, Journal of the Taiwan Institute of Chemical Engineers, Volume 104, 2019, Pages 40-53, ISSN 1876-1070, https://doi.org/10.1016/j.jtice.2019.09.018.

[30] Hossein Nami, Faramarz Ranjbar, Mortaza Yari, Methanol synthesis from renewable H_2 and captured CO_2 from S-Graz cycle – Energy, exergy, exergoeconomic and exergoenvironmental (4E) analysis, International Journal of Hydrogen Energy, Volume 44, Issue 48, 2019, Pages 26128-26147, ISSN 0360-3199, https://doi.org/10.1016/j.ijhydene.2019.08.079.

[31] Kuo Chen, Jian Yu, Bin Liu, Congcong Si, Hongyan Ban, Weijie Cai, Congming Li, Zhong Li, Kaoru Fujimoto, Simple strategy synthesizing stable CuZnO/SiO2 methanol synthesis catalyst, Journal of Catalysis, Volume 372, 2019, Pages 163-173, ISSN 0021-9517, https://doi.org/10.1016/j.jcat.2019.02.035.

[32] Shashwata Ghosh, Srinivas Seethamraju, Feasibility of reactive distillation for methanol

synthesis, Chemical Engineering and Processing - Process Intensification, Volume 145, 2019, 107673, ISSN 0255-2701, https://doi.org/10.1016/j.cep.2019.107673.

[33] Nima Norouzi, Maryam Fani, Zahra Karami Ziarani, The fall of oil Age:A scenario planning approach over the last peak oil of human history by 2040, Journal of Petroleum Science and Engineering, Volume 188, 2020, 106827, ISSN 0920-4105, https://doi.org/10.1016/j.petrol.2019.106827.

[34] Norouzi, N.; Talebi, S. "An Overview on the Green petroleum Production". Chemical Review and Letters. Volume 4 ,2020, 9-15, https://dx.doi.org/10.22034/crl.2020.222515.1041

[35] Hosseinpour M, Fatemi S, Ahmadi SJ, Morimoto M, Akizuki M, Oshima Y, Fumoto E. The synergistic effect between supercritical water and redox properties of iron oxide nanoparticles during in-situ catalytic upgrading of heavy oil with formic acid. Isotopic study. Applied Catalysis B: Environmental 2018:230:91-101.

[36] Hosseinpour M, Fatemi S, Ahmadi SJ, Oshima Y, Morimoto M, Akizuki M. Isotope tracing study on hydrogen donating capability of supercritical water assisted by formic acid to upgrade heavy oil: Computer simulation vs. experiment. Fuel 2018: 225:161-173.

[37] Hosseinpour M, Golzary A, Saber M, Yoshikawa K. Denitrogenation of biocrude oil from algal biomass in high temperature water and formic acid mixture over H+ ZSM-5 nanocatalyst. Fuel 2017:206:628-637.

[38] Hosseinpour M, Akizuki M, Oshima Y, Soltani M. Influence of formic acid and iron oxide nanoparticles on active hydrogenation of PAHs by supercritical water. Isotope tracing study. Fuel 2019:254:115675.

[39] Huifang Li, Jiachen Liang, Huan Li, Xiaoyu Zheng, Ying Tao, Zheng-Hong Huang, Quan-Hong Yang, Activated carbon fibers with manganese dioxide coating for flexible fiber supercapacitors with high capacitive performance, Journal of Energy Chemistry, Volume 31, 2019, Pages 95-100.

[40] Hui Kong, Xianghui Kong, Hongsheng Wang, Jian Wang, A strategy for optimizing efficiencies of solar thermochemical fuel production based on nonstoichiometric oxides, International Journal of Hydrogen Energy, Volume 44, Issue 36, 2019, Pages 19585-19594.